ibid. 30B, 494 (1969).

[8]We are grateful to Dr. K.-W. Lai and Dr. Paul Hoch for generously providing the necessary distributions from their unpublished data.

[9]This subject has been reviewed by J. L. Rosner, in *Experimental Meson Spectroscopy*, edited by C. Baltay and A. H. Rosenfeld (Columbia Univ. Press, 1970), p. 499; and by C. W. Akerlof, University of Michigan report, 1970 (unpublished).

[10]D. Birnbaum, R. M. Edelstein, N. C. Hien, T. J. McMahon, J. F. Mucci, J. S. Russ, E. W. Anderson, E. J. Bleser, H. R. Blieden, G. B. Collins, D. Garelick, J. Menes, and F. Turkot, Phys. Letters 31B, 36 (1970), and references cited therein.

[11]For one possible exception, see G. Yekutieli, D. Yaffe, S. Toaff, A. Shapira, E. E. Ronat, U. Karshon, B. Haber, and Y. Eisenberg, Phys. Rev. Letters 25, 184 (1970). However, see also E. Berger and R. Morrow, *ibid.* 25, 1136 (1970).

[12]Dahl *et al.*, Ref. 2.

[13]C. Quigg, Nucl. Phys. B (to be published); F. S. Henyey, G. L. Kane, and J. J. G. Scanio, Phys. Rev. Letters 27, 350 (1971).

[14]C. W. Akerlof, P. K. Caldwell, C. T. Coffin, P. Kalbaci, D. I. Meyer, P. Schmueser, and K. C. Stanfield, Phys. Rev. Letters 27, 539 (1971).

PHYSICAL REVIEW D VOLUME 4, NUMBER 9 1 NOVEMBER 1971

Photoproduction of Neutral ρ Mesons*

G. McClellan,† N. Mistry, P. Mostek,‡ H. Ogren,§ A. Silverman, J. Swartz,|| and R. Talman
Laboratory of Nuclear Studies, Cornell University, Ithaca, New York 14850
(Received 27 May 1971)

Results are presented on a series of measurements of ρ-photoproduction from hydrogen, deuterium, and complex nuclei ranging up to lead, at photon energies ranging from 4 to 9 GeV. Detailed dipion mass-spectrum fits are presented, using a Drell-type nonresonant background and its interference with the resonant amplitude, with no other arbitrary backgrounds. For hydrogen and deuterium, the inelastic contributions have been subtracted. The A dependence of the cross sections is analyzed to yield values of $\gamma_\rho{}^2/4\pi$ and $\sigma_{\rho N}$ at average photon energies of 6.1, 6.5, and 8.8 GeV. The hydrogen-to-deuterium ratios indicate the presence of possible nondiffractive amplitudes at low energies which then decrease with energy.

I. INTRODUCTION

Results are presented on a series of measurements on ρ^0 photoproduction from elements ranging from hydrogen to lead, at average photon energies ranging from 4 to 9 GeV. Some of the data in the present analysis were presented in previous publications.[1] These data have been reanalyzed using a consistent scheme of analysis for all the sets of data. In no case have the cross sections reported in Ref. 1 been changed by more than 9%. However, due mainly to the inclusion of the real part of the ρN scattering amplitude, the values of $\gamma_\rho{}^2/4\pi$ and $\sigma_{\rho N}$ extracted from the data have changed by about 35%. Here $\gamma_\rho{}^2/4\pi$ is the direct ρ^0-photon coupling constant and $\sigma_{\rho N}$ the total ρ^0 cross section on a free nucleon.

Dipion mass spectra were measured in detail for several representative nuclei at three energies, 4.4, 6.5, and 8.8 GeV. These mass spectra have been fitted in the mass range ~500 to ~1000 MeV using an interference model[2] and no arbitrary background subtractions. Parameters obtained from these representative fits are found to be fairly independent of the target element at any particular energy, and these parameters are then used for all elements at the same energy to extract the 0° ρ^0-photoproduction cross sections.

The A dependences of the 0° cross sections at each energy (using the elements from deuterium to lead) are then fitted using an optical-model calculation with $\gamma_\rho{}^2/4\pi$ and $\sigma_{\rho N}$ as free parameters. Two sets of nuclear parameters are used in two independent sets of fits: (i) nuclear radii determined by fitting total nucleon-nucleus cross sections[3] using a consistent optical model, and (ii) nuclear parameters measured by electron-scattering experiments.[4] This second set of parameters agrees well with nuclear parameters determined from high-energy proton-nucleus scattering using an optical-model analysis[5] closely related to the present analysis. The results of these fits using the two different sets of parameters differ from each other by less than 10%. The effective photoproduction cross section from *single nucleons* is obtained from these fits and may be compared with the measured hydrogen cross sections in the same energy range.

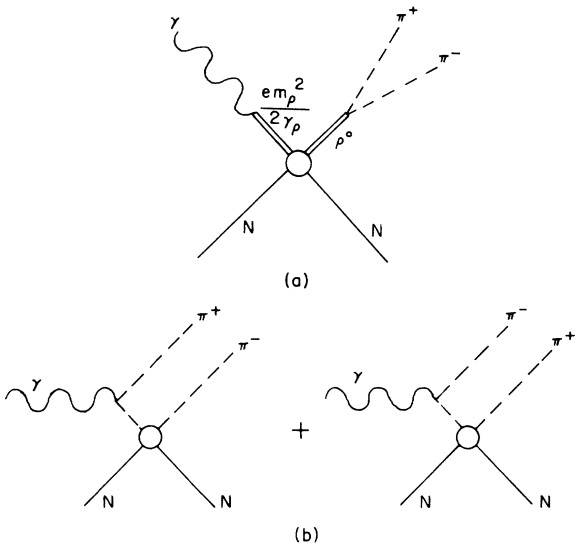

FIG. 1. Processes contributing to $\pi^+\pi^-$ pairs in the ρ^0 region. (a) The ρ-dominance picture. (b) The "Drell" process where one pion scatters diffractively from the target. For complex nuclei, one has to include terms where both pions can scatter from the nucleus.

II. DATA ANALYSIS AND RESULTS

A. Mass Spectra; Extraction of Cross Sections

The pair spectrometer used to detect the $\pi^+\pi^-$ pair has been described previously.[1] Typical acceptances [full width at half maximum (FWHM)] are $\Delta m_{\pi\pi}/m_{\pi\pi}=\pm 4\%$ and $\Delta p_\rho/p_\rho=\pm 7\%$. (Hydrogen and deuterium measurements at 6.1 and 6.5 GeV used an acceptance $\Delta p_\rho/p_\rho=\pm 20\%$.)

In the absence of any precise theory of the line shape of broad resonances like the ρ^0, we have analyzed the dipion mass spectra in the following way. We consider the dipion production to be dominated by a p-wave relativistic resonance,[6] the ρ^0 meson, Fig. 1(a); we include nonresonant production via a "Drell" process as shown in Fig. 1(b), and an interference term between the two processes as suggested by Söding.[2] We include no other arbitrary background processes. In the case of complex nuclei, the Drell amplitude has to be worked out in detail allowing for the case where *both* pions may be scattered off the nucleus. For the present we have used the naive picture in Fig. 1(b) but inserted a numerical factor A_0 for this effect as calculated by Bauer.[7]

Detailed mass spectra at fixed energy have been measured at $\langle E_\rho\rangle = 4.4$ GeV for deuterium, carbon, copper, and lead; at $\langle E_\rho\rangle = 6.5$ GeV for carbon and copper; and at $\langle E_\rho\rangle = 8.8$ GeV for carbon, copper, and lead.

We fit these spectra using the "model" outlined above, with the following quantities as parameters of the fit:

(i) Γ_0 (MeV), the "width" of the ρ^0 resonance at $m_{\pi\pi}=m_\rho$,

(ii) C_A, a coefficient multiplying the interference term,

(iii) $d\sigma/d\Omega_\rho(t=0)$, the ρ^0-photoproduction cross section.

The mass m_0 of the ρ meson is fixed to be 775 MeV, which is a close approximation to the value given by the colliding-beam experiments in their analysis considering ρ-ω interference. The absolute value of the Drell term is fixed, since we use measured pion-nucleus total cross sections in the calculation. As mentioned above, we include a factor A_0, which varies smoothly from 0.48 for beryllium to 0.34 for lead (see Table I). It should be noted that the Drell amplitude includes a factor $(m_\rho^2 - m_{\pi\pi}^2)/(m_\rho^2 - m_{\pi\pi}^2 + im_\rho\Gamma)$ which accounts for the "domination" of the dipion production by the ρ^0 resonance and thus avoids "double counting."[8] We allow the coefficient of the interference term, C_A,

TABLE I. Fits to the dipion mass spectra. The three fitting parameters are Γ_0, $(d\sigma/d\Omega)_\rho$, and C_A. A_0 is a factor reducing the Drell cross section in complex nuclei. (See Ref. 7.) The last column gives values of χ^2 divided by the number of degrees of freedom.

Element	E_ρ (GeV)	m_ρ (MeV)	Γ_0 (MeV)	$(d\sigma/d\Omega)_\rho(t=0)$ (b/sr)	C_A	A_0	$\chi^2/(N-3)$
C	8.8	775	118± 6	0.236±0.01	0.61±0.04	0.45	3.2
Cu	8.8	775	113± 9	4.91 ±0.24	0.43±0.05	0.39	5.6
Pb	8.8	775	124± 5	26.9 ±0.9	0.47±0.04	0.34	2.1
C	6.5	775	126± 5	0.139±0.004	0.64±0.03	0.45	1.3
Cu	6.5	775	122± 7	2.75 ±0.08	0.57±0.03	0.39	2.9
D	4.4	775	130±18	0.003±0.0003	0.57±0.06	0.56	2.5
C	4.4	775	142± 7	0.085±0.003	0.73±0.03	0.45	1.4
Cu	4.4	775	142±11	1.40 ±0.10	0.49±0.09	0.39	1.7
Pb	4.4	775	114± 7	7.36 ±0.32	0.63±0.06	0.34	3.5

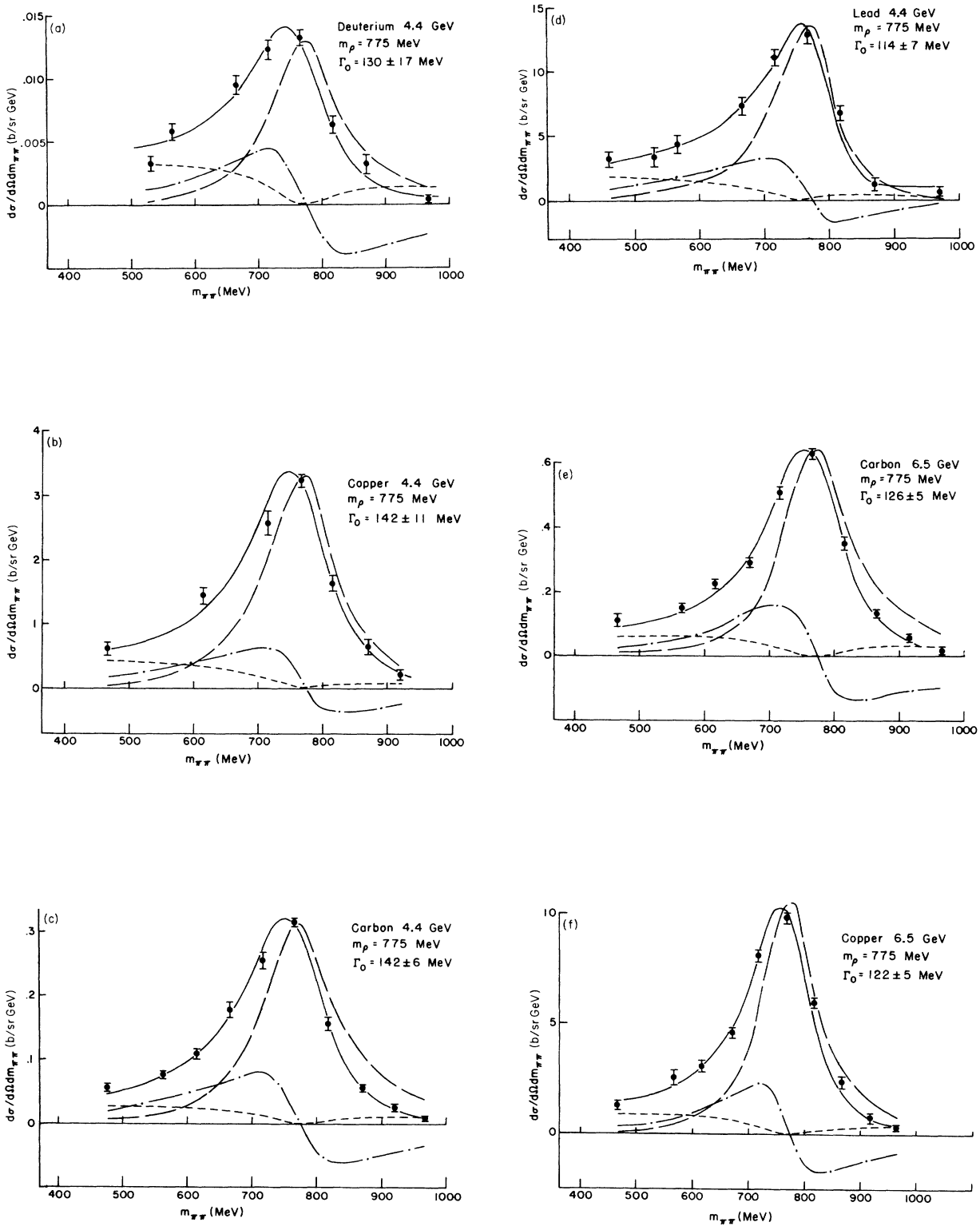

FIG. 2. *(Continued on next page.)*

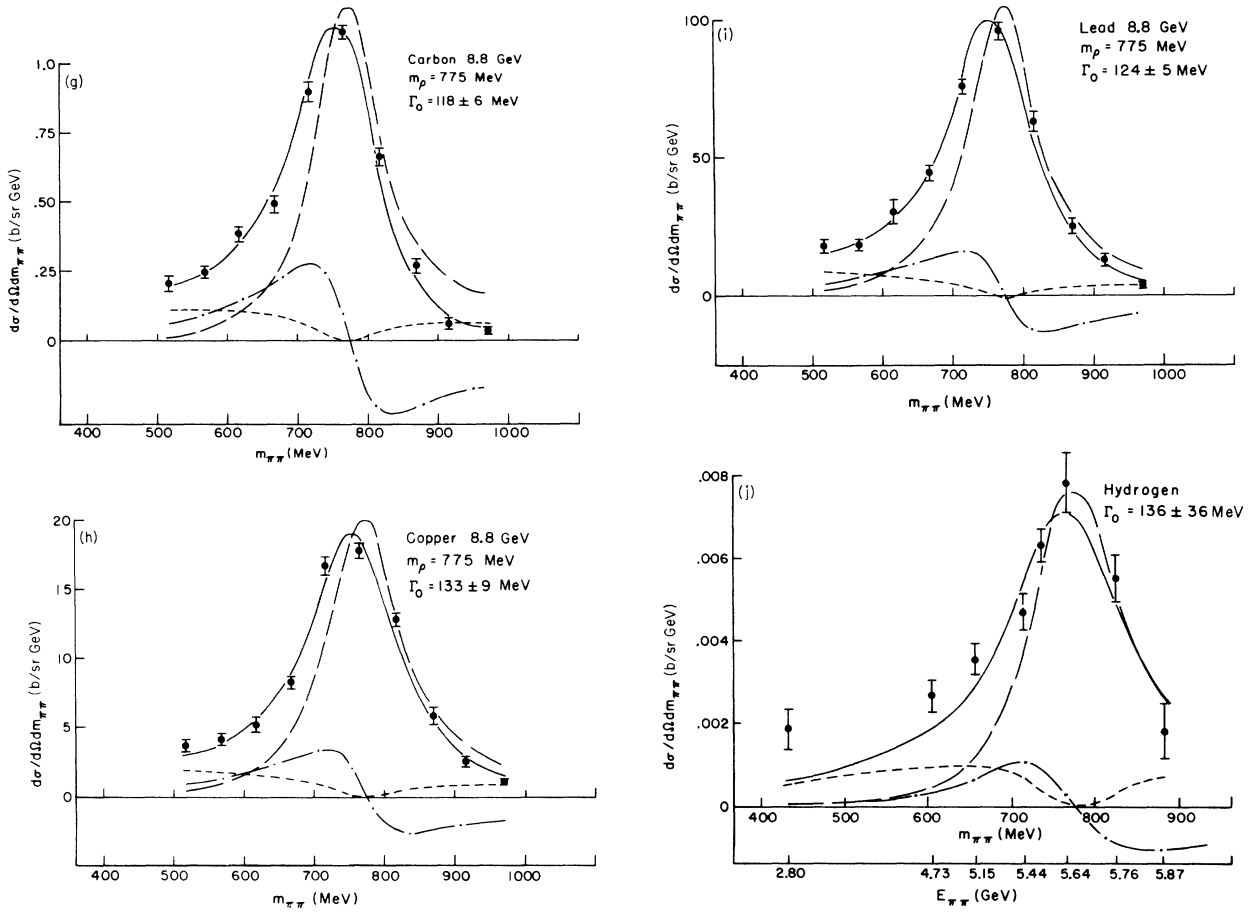

FIG. 2. Dipion mass spectra from various elements at three different energies. The long-dashed curve shows the Breit-Wigner resonance contribution; the short-dashed curve is the square of the Drell term; the dot-dashed curve is the Söding interference term between the two. The smooth curve is the best fit to the data obtained by integration of the above three terms over the mass acceptance of the spectrometer.

to be a parameter, since the relative phase between the Drell process and the ρ^0-production amplitudes may vary with nuclear size.

Fits to the mass spectra are shown in Fig. 2 and all the relevant parameters are listed in Table I. The results indicate an average width Γ_0 which is larger at 4.4 GeV than at the higher energies 6.5 and 8.8 GeV. The average width from the 6.5- and 8.8-GeV data is $\Gamma_0 = 124 \pm 4$ MeV, which is in good agreement with the best width from the Orsay colliding-beams result.[9] The larger value of Γ_0 for the 4.4-GeV spectra may be an indication that the particular model chosen for analysis may not be appropriate.

For hydrogen, mass spectra were measured in the early stages of the experiment, using fixed geometry and scaling the field in both magnets to vary the mass and thus the energy E_ρ as well. These spectra are fit with the same procedure as outlined above, except that an energy-dependent form of the ρ production is introduced to fit the general energy dependence of $d\sigma/dt(\gamma + p \to \rho^0 + p)$ at $t = 0$ shown by this and other experiments. Thus $(d\sigma/dt)_{t=0} = \text{const}(1 + 1.3/p_\rho)^2$. Similarly, the energy dependence of the πp total cross section is used in the Drell terms, i.e., $\sigma_{\pi p} = 24(1 + 0.8/p_\pi)$ mb. A typical fit to the data is shown in Fig. 2(j).

The parameters obtained in these various mass fits have to be used now to extract the cross section $(d\sigma/dt)_\rho$ for those elements where only a single mass point was measured, usually at $m_{\pi\pi} \sim 760$ MeV. We note that the "background" terms are both explicitly zero at the central mass of the Breit-Wigner resonance, i.e., at $m_{\pi\pi} = 775$ MeV. Thus, a measurement of $d^2\sigma/d\Omega dm$ with a narrow mass acceptance centered at 775 MeV would need no background subtraction, and could be multiplied by the appropriate normalization to obtain $(d\sigma/dt)_\rho$, if the width Γ_0 were known. For measurements of $d^2\sigma/d\Omega dm$ at $m_{\pi\pi} \sim 760$ MeV with a finite mass acceptance, we need a procedure for the necessary small subtraction. This is done by using the ratio

$R_\rho(m_{\pi\pi})$ of the resonance contribution to the fitted cross section $d^2\sigma(m_{\pi\pi})/d\Omega dm$ for each element at each energy. For complex nuclei $R_\rho(m_{\pi\pi})$ is independent of energy and element for the mass range $700 < m_{\pi\pi} < 850$ MeV which covers the mass acceptance for a typical data point at the "peak." For hydrogen and deuterium, $R_\rho(m_{\pi\pi})$ was obtained separately at $\langle E_\rho \rangle = 4.4$, 5.6, and 7.5 GeV, and was found to be independent of energy. Cross sections $(d\sigma/dt)_\rho$ are then obtained from the counting rate using a computer efficiency program that includes a $\sin^2\theta_\pi^*$ weighting for the pion decay angle in the ρ rest system and an extrapolation to $\theta_\rho = 0$ determined by an optical model using the appropriate nuclear parameters, as described in Sec. III C below.

Table II lists, for deuterium and heavier nuclei, the measured $d^2\sigma/d\Omega dm_{\pi\pi}$ and values of $(d\sigma/dt)_\rho$ averaged over the aperture, obtained by leaving out the optical-model extrapolations to $\theta_\rho = 0$. The next two columns list the derived values $(d\sigma/dt)_{\theta=0}$, using optical-model extrapolations to $\theta = 0$ with the two sets of nuclear radii. In the case of the heavier nuclei, appreciable corrections need to be made to the measured cross sections. However it is apparent that the two different sets of nuclear parameters lead to the same results.

B. Hydrogen and Deuterium Cross Sections

Figure 3 shows the t dependence of the hydrogen and deuterium cross sections, at average energies $\langle E_\rho \rangle = 7.3$ and 5.5 GeV. These cross sections have been corrected for inelastic ρ^0 production using calculations of Wolf.[10] Preliminary results of the inelastic contribution, measured by using a proton-recoil hodoscope in coincidence with the pair spectrometer described above, are in reasonable agreement with the values given by Wolf. The resulting subtraction amounts to 4% at $\theta = 0$ for hydrogen. For deuterium, the inelastic cross section is taken to be twice that for hydrogen and the data are corrected accordingly. The coherent forward peak for deuterium is clearly seen. In the "incoherent" region where $|t| > 0.1$ (GeV/c)^2, the deuterium t dependence is the same as that of hydrogen.

If one writes $d\sigma/dt = Ae^{bt}$, then for hydrogen $b = 9.0 \pm 0.6$ (GeV/c)$^{-2}$ at 7.3 GeV and $b = 8.6 \pm 0.5$ (GeV/c)$^{-2}$ at 5.5 GeV. These data represent measurements mainly at the "peak" of the ρ mass shape. Detailed mass spectra were not measured

TABLE II. Differential cross sections (averaged over aperture): $\langle d^2\sigma/dmd\Omega \rangle$ are the measured cross sections at the "peak" of the ρ production, with just the efficiency of the apparatus divided out; $\langle (d\sigma/dt)_\rho \rangle$ are the integrated cross sections, using $\Gamma_0 = 124$ MeV and with nonresonant subtractions as obtained from the mass-spectrum fits. $d\sigma/dt(\theta = 0)$ are the corresponding cross sections extrapolated to $\theta = 0$ using an optical model with the relevant parameters.

E_ρ (GeV)	Element	$\langle d^2\sigma/d\Omega dm \rangle$ (b sr^{-1}GeV^{-1})	$\langle (d\sigma/dt)_\rho \rangle$ (mb GeV^{-2})	$(d\sigma/dt)_{\theta=0}$ (mb GeV^{-2}) Best fit	E-S
8.8	D	0.0441 ± 0.0014	0.333 ± 0.011	0.362 ± 0.011	0.362 ± 0.011
	Be	0.549 ± 0.014	4.72 ± 0.12	5.41 ± 0.13	5.35 ± 0.13
	C	0.894 ± 0.015	7.65 ± 0.13	8.70 ± 0.15	8.84 ± 0.15
	Mg	2.67 ± 0.07	25.1 ± 0.61	31.2 ± 0.8	31.7 ± 0.8
	Cu	10.7 ± 0.3	92.3 ± 2.3	133 ± 3	131 ± 3
	Ag	21.6 ± 0.5	185 ± 5	300 ± 8	288 ± 7
	In	24.5 ± 0.6	211 ± 6	346 ± 9	332 ± 9
	Au	43.1 ± 1.1	374 ± 9	719 ± 18	674 ± 17
	Pb	47.1 ± 1.3	410 ± 12	804 ± 23	752 ± 21
6.5	D	0.0283 ± 0.0012	0.424 ± 0.017	0.438 ± 0.018	0.438 ± 0.018
	C	0.527 ± 0.017	8.28 ± 0.27	8.74 ± 0.28	8.77 ± 0.28
	Mg	1.81 ± 0.07	28.5 ± 1.1	31.3 ± 1.2	31.5 ± 1.2
	Cu	6.62 ± 0.23	103 ± 3	121 ± 4.0	121 ± 4.0
	Ag	13.7 ± 0.5	217 ± 8	265 ± 9.1	261 ± 9.0
	Pb	30.6 ± 1.2	482 ± 19	635 ± 25	617 ± 25
6.1	D	0.0197 ± 0.009	0.398 ± 0.016	0.403 ± 0.017	0.403 ± 0.017
	Be	0.278 ± 0.010	4.86 ± 0.15	5.69 ± 0.17	5.57 ± 0.17
	C	0.473 ± 0.014	8.27 ± 0.25	9.51 ± 0.28	9.61 ± 0.28
	Mg	1.34 ± 0.041	23.5 ± 0.72	29.4 ± 0.9	30.2 ± 0.9
	Cu	5.15 ± 0.15	90.3 ± 2.6	133 ± 4	129 ± 4
	Ag	9.60 ± 0.30	168 ± 5	277 ± 8	265 ± 9
	Au	16.2 ± 0.5	283 ± 9	569 ± 18	517 ± 16
	Pb	16.8 ± 0.6	296 ± 10	604 ± 20	552 ± 18

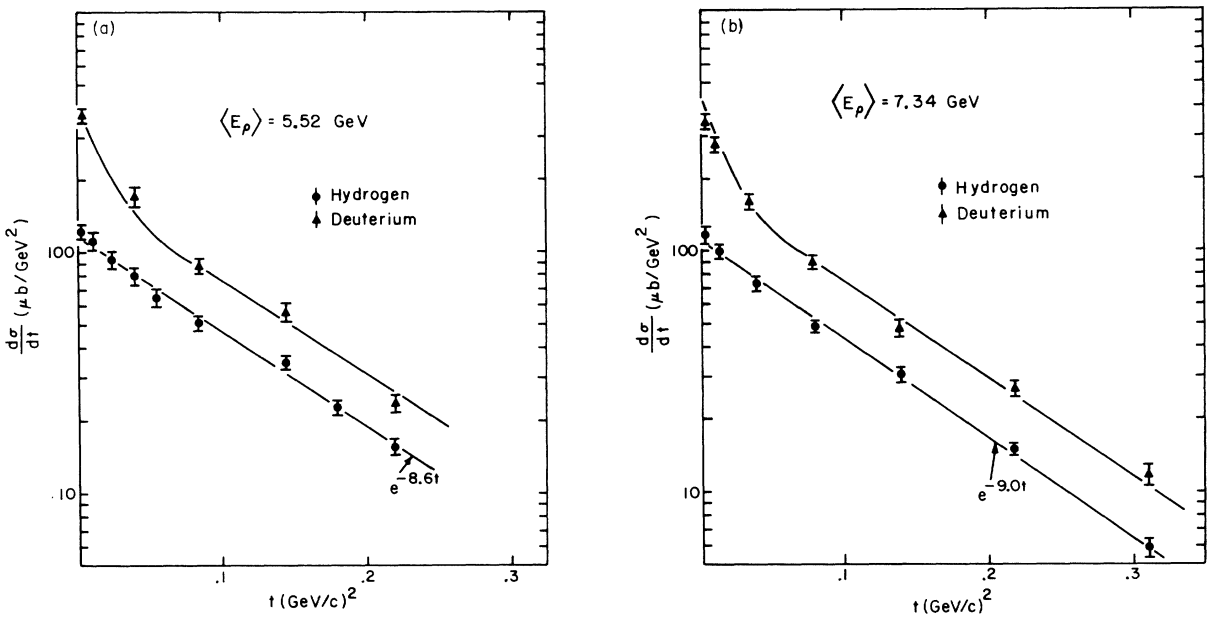

FIG. 3. The t dependence of the hydrogen and deuterium cross sections $d\sigma/dt$ at (a) 5.52 GeV and (b) 7.34 GeV.

at large t; it is possible that the t dependence of the Drell-type amplitude and interference terms may affect the results.

Note added in proof. Preliminary results[10a] from measurements of the ρ^0 line shape in elastic ρ^0 photoproduction at 8.5 GeV from hydrogen, at t values up to -0.5 (GeV/c)^2, indicate that the t dependence of the extracted Drell cross section is in excellent agreement with the theoretical prediction: $D(t) \sim (1 + q_\pi{}^2/m_\pi{}^2)^{-2}\exp(9t + 2.4t^2)$, where $q_\pi{}^2$ is the square of the four-momentum of the virtual pion. The resultant "elastic" ρ^0 cross section is $(d\sigma/dt)_H = 103\ \exp(8.1t)\ \mu$b/GeV^2.

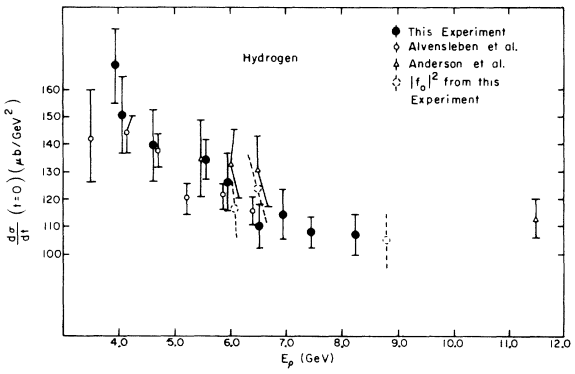

FIG. 4. The hydrogen cross sections $d\sigma/dt$ at $t = 0$ as a function of energy E_ρ. Data from DESY (Ref. 11) and SLAC (Ref. 13) are included. Also shown are three points representing $|f_0|^2$ obtained in the present experiment from A-dependence fits.

Table III lists the $t = 0$ cross sections for hydrogen and deuterium at various average energies $\langle E_\rho \rangle$. Figure 4 shows the hydrogen cross section as measured by several experimental groups[11,12,13] and includes the present results. Also shown are three points representing the "single-nucleon" cross section $|f_0|^2$ resulting from the fits to the A dependence of the present data, at $\langle E_\rho \rangle = 6.1$, 6.5, and 8.8 GeV. The general trend of the hydrogen cross sections shows a gradual decrease with energy up to about 6 GeV and then a leveling off at a cross section of about 102 ± 10 μb/GeV^2.

In Fig. 5 the ratio of the deuterium and hydrogen cross sections at $t = 0$, $R_{DH}(t = 0)$, is plotted as a

TABLE III. Energy dependence of the hydrogen and deuterium cross sections $d\sigma/dt$ at $t = 0$, and the ratio $R_{DH} \equiv (d\sigma/dt)_{\text{deuterium}}/(d\sigma/dt)_{\text{hydrogen}}$ at $t = 0$.

	$(d\sigma/dt)_{t=0}$		
E_ρ (GeV)	Hydrogen (μb/GeV^2)	Deuterium (μb/GeV^2)	R_{DH}
3.91	169 ± 14	470 ± 20	2.78 ± 0.28
4.08	150 ± 14	447 ± 21	2.98 ± 0.32
4.61	140 ± 13	432 ± 24	3.09 ± 0.34
5.58	134 ± 6	431 ± 11	3.22 ± 0.16
5.92	126 ± 9	402 ± 19	3.20 ± 0.28
6.53	109 ± 9	392 ± 20	3.59 ± 0.34
6.94	113 ± 10	417 ± 20	3.69 ± 0.34
7.40	108 ± 4.5	387 ± 12	3.58 ± 0.18
8.24	107 ± 7	323 ± 14	3.02 ± 0.24
8.80		358 ± 20	

function of energy. At energies below 6 GeV, the ratio is significantly lower than the prediction of the Glauber theory (straight line in Fig. 5) but is quite consistent with predictions above ~6 GeV. (Here we have used a constant value $\sigma_{\rho N} = 29$ mb in the Glauber multiple-scattering correction.) The discrepancy from the predicted value can be used to indicate the presence of $I = 1$ isospin exchange in the nucleon amplitude. A somewhat detailed explanation of the reasoning has been published previously[1] and will not be repeated here. The energy dependence of the discrepancy may be of the form (S^{-1}). Such a curve is shown in Fig. 5 as an example.

C. Complex Nuclei: Optical-Model Fits

The cross sections $(d\sigma/dt)_{\theta=0}$ listed in Table II are used in a two-parameter fit with an "optical-model" calculation described below. Separate fits are made for each set of data at a particular average energy and each set of nuclear parameters as described below.

The coherent part of the cross section at $\theta = 0$ for an element A is written in terms of the single-nucleon cross section at $t = 0$, $|f_0|^2$, times the square of the "effective number of nucleons," $N_{\rm eff}{}^2(A)$. The vector-dominance model is used to write $|f_0|^2$ in terms of the direct photon-ρ^0 coupling $\gamma_\rho{}^2/4\pi$ (we neglect the contribution from γ-ω^0 and γ-ϕ^0 direct couplings) and the ρ-nucleon scattering cross section $[d\sigma(0)/dt]_{\rho N}$ at $t = 0$.

Thus

$$|f_0|^2 = \frac{\alpha}{4}\left(\frac{4\pi}{\gamma_\rho{}^2}\right)\left[\frac{d\sigma(0)}{dt}\right]_{\rho N} = \frac{\alpha}{4}\left(\frac{4\pi}{\gamma_\rho{}^2}\right)\frac{1}{16\pi}\sigma_{\rho N}{}^2\,(1+\alpha_{\rho\rho}{}^2), \tag{1}$$

where $\alpha_{\rho\rho}$ is the ratio of the real to the imaginary part of the ρ^0-nucleon scattering amplitude. $\alpha_{\rho\rho}(k_\gamma)$ is taken to be the same as that given by analysis of the total photon-nucleon cross sections[14]; this is consistent with the assumption of ρ dominance in photon interactions. In particular, the values of $\alpha_{\rho\rho}$ used at each energy are listed in Table V; these are the values given by using the curve labeled $(A\&B)$ in Ref. 14.

The parameters of the fit are then $\gamma_\rho{}^2/4\pi$ and $\sigma_{\rho N}$ at each energy, and for each set of nuclear parameters.

We have estimated the contribution at $\theta = 0$ due to incoherent production from single nucleons as outlined by Trefil.[15] For beryllium and all heavier nuclei, we find the contribution to be negligible. Thus the cross sections $d\sigma/dt(0°)$ of Table II are fit directly by the coherent part of the calculated cross section for nuclei larger than deuterium. For deuterium, $N_{\rm eff}{}^2$ is calculated using the "closure" approximation, and thus includes the incoherent production.

We give below the complete expression for $N_{\rm eff}{}^2$ for nuclei larger than deuterium:

$$N_{\rm eff}{}^2 = \left| 2\pi \int_0^\infty b^2 db \int_{-\infty}^{\infty} dz\, J_0(b, q_\perp) e^{i\Delta z} \rho_c(\vec{b}, z) \times \exp\left(\frac{-\sigma}{2}(1-\alpha_{\rho\rho})\int_z^\infty \rho_c(\vec{b}, z')dz'\right)\right|^2, \tag{2}$$

where b = impact parameter; $q_\perp$ = transverse momentum transfer to the nucleus; $J_0(b, q_\perp)$ = Bessel function of zeroth order, arising from the nuclear shape; Δ = longitudinal momentum transfer, due to the unequal masses of the ρ and photon, $\Delta = m_\rho{}^2/2k$; $\alpha_{\rho\rho}$ = real/imaginary ratio of the ρ-nucleon amplitude; $\sigma = \sigma_{\rho N}$, the ρ-nucleon total cross section; and $\rho_c(b, z)$ is the nuclear density distribution integrated over the range of the ρ-nucleon interaction and includes the effect of two-particle correlations within the nucleus.

We summarize here the main features of the estimation of correlation effects, due to Bauer.[7] We use a Gaussian form for the two-particle correlation function, of range inversely proportional to $n^{1/3}$, where n is the local nucleon number density. Thus the correlation function $g(\vec{s}, z')$ is normalized for Fermi statistics:

$$\int ds^2 dz' g(\vec{s}, z') = \frac{-1}{n(\vec{b}, z)}, \tag{3}$$

where $\vec{s}$ and z' are the relative-distance parameters. Also, $g(0) = -\frac{1}{4}$ since we have protons and neutrons each with two spin states. We use no

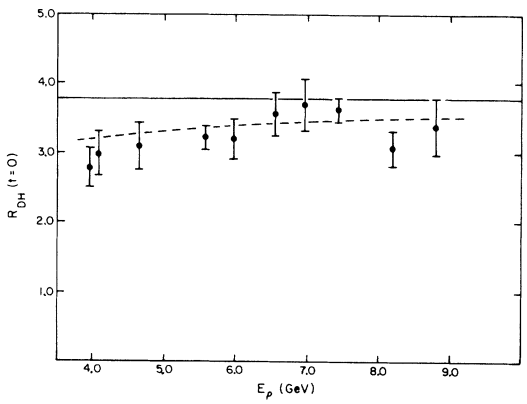

FIG. 5. The ratio $R_{\rm DH}$, $(d\sigma/dt)_{\rm deuterium}/(d\sigma/dt)_{\rm hydrogen}$, at $t = 0$ for various energies. The straight line at $R_{\rm DH} = 3.77$ represents the prediction for pure diffractive photoproduction. The dashed curve represents an arbitrary S^{-1} fit, where $S \simeq 2kM_p$ = total c.m. energy squared.

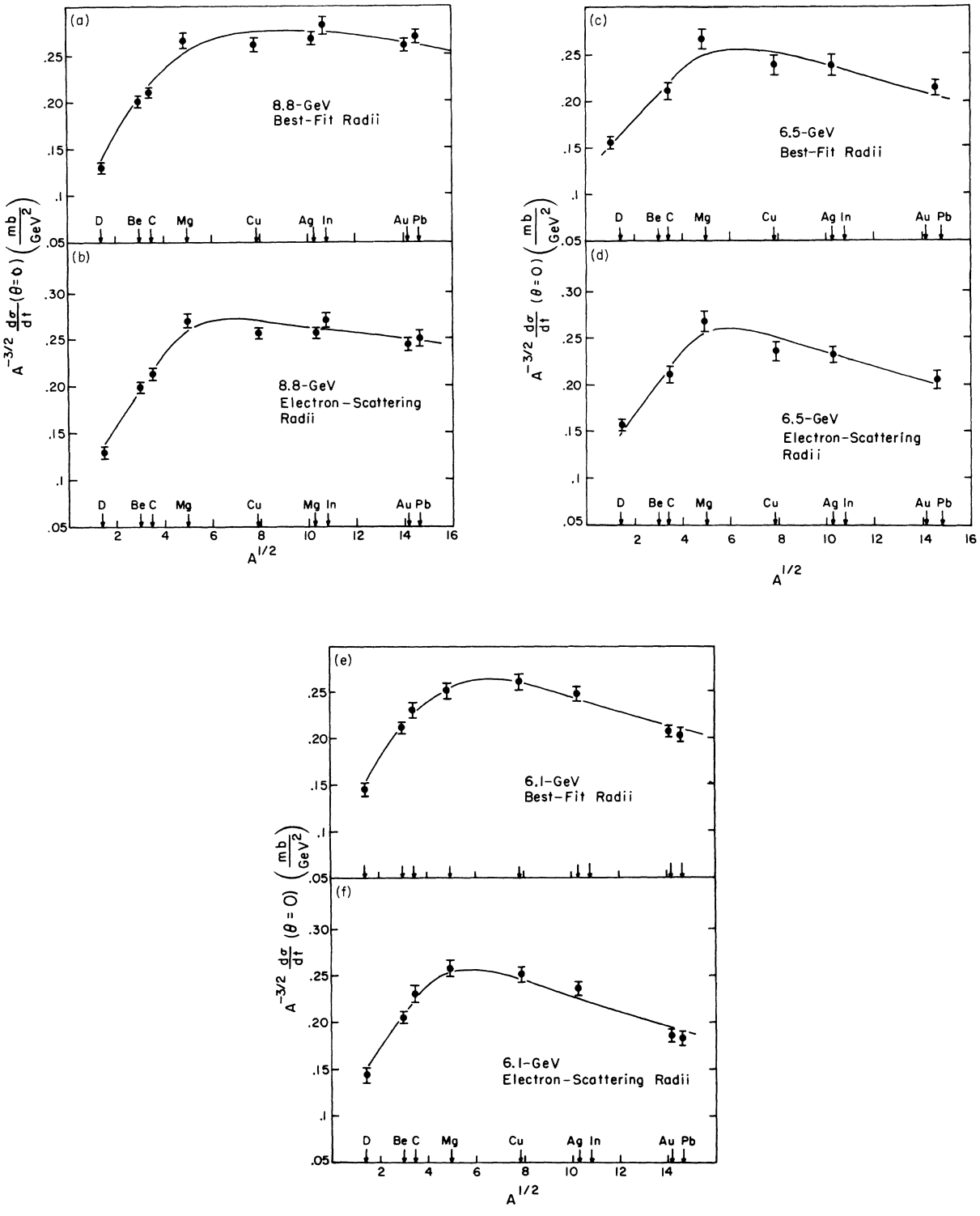

FIG. 6. Optical-model fits to the A dependence of cross sections $d\sigma/dt$ at $\theta=0$ for the two sets of nuclear parameters. Best-fit and E-S at three energies: (a) and (b) at 8.8 GeV; (c) and (d) at 6.5 GeV; (e) and (f) at 6.1 GeV.

hard-core repulsion, since the effect of "smearing" over the nucleon form factor reduces the effect of the core. We now assume that the main contribution to ρ production comes from the edge of the nucleus because of the expected strong absorption of the ρ. Thus due to the low surface density, the range of correlations is much larger than the nucleon-form-factor "range," and in this approximation we estimate the correlation length ξ to be given by

$$\xi(\vec{b}, z) \simeq (4^{1/3}/16)[n(\vec{b}, z)]^{-1/3}. \quad (4)$$

The nuclear density with correlations included is then given by

$$\rho_c(\vec{b}, z) = \rho(\vec{b}, z)[1 + \sigma\xi\rho(\vec{b}, z)], \quad (5)$$

where $\rho(\vec{b}, z)$ is the nucleon number density integrated over the nucleon form factor $f(t) = f(0)e^{a_0 t}$, $t \equiv -q^2$, $a_0 \simeq 5$ (GeV/c)$^{-2}$. Thus,

$$\rho(\vec{b}, z) = \int d^2s\, n(\vec{s}, z)\, \frac{1}{4\pi a_0} \exp\left(\frac{-|\vec{b} - \vec{s}|^2}{4a_0}\right). \quad (6)$$

For the nucleon number density $n(r)$ we have used a harmonic-oscillator shell-model distribution for beryllium and carbon:

$$n(r) = n_0(1 + \delta r^2/a_0^2)\exp(-r^2/a_0^2), \quad (7)$$

where $\delta = \frac{4}{3}$ for carbon and $\frac{5}{6}$ for beryllium. a_0 is a parameter of the fit. For all heavier nuclei ($A > 12$) we use the Woods-Saxon distribution

$$n(r) = n_0\{1 + \exp[(r - c)/\epsilon]\}^{-1}, \quad (8)$$

where c is the half-density radius and 4.4ϵ is the "skin thickness."

The two sets of nuclear parameters are listed in Table IV. The "best-fit" parameters are obtained by using an optical model similar to that used for

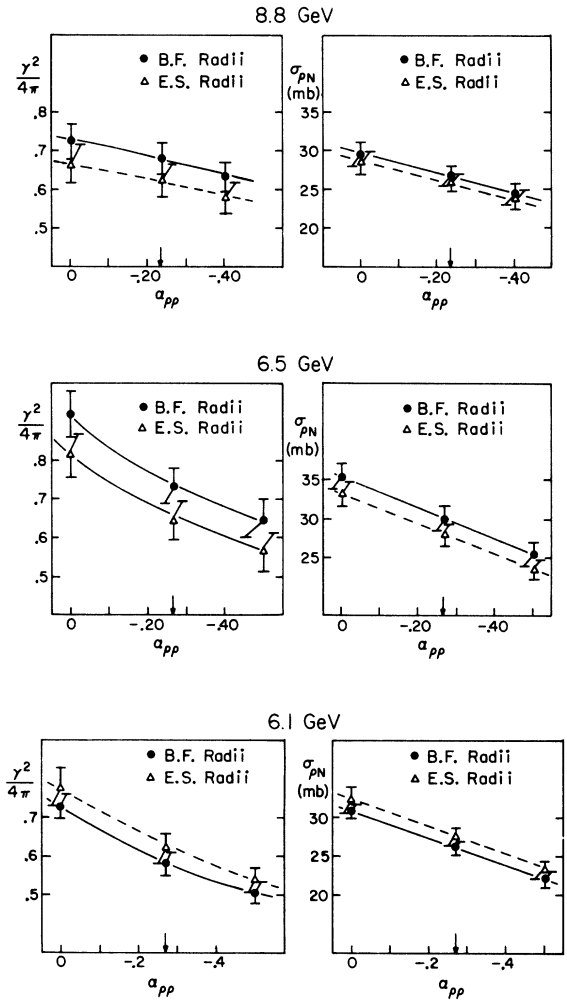

FIG. 7. Variation of the parameters $\gamma_\rho^2/4\pi$ and $\sigma_{\rho N}$ with $\alpha_{\rho\rho}$.

TABLE IV. Nuclear parameters for the two sets labeled best fit and E-S. The density distributions are given in Eqs. (2) and (3) in the text. The parameter ϵ was fixed at 0.545 fermi for the best-fit set.

	Best-fit parameters			E-S parameters		
Element	a_0 (F)	$a_{\rm rms}A^{-1/3}$ (F)		a_0 (F)	$a_{\rm rms}A^{-1/3}$ (F)	
Be	1.64 ± 0.07	1.11		1.56	1.06	
C	1.50 ± 0.04	0.96		1.61	1.03	
	c (F)	$cA^{-1/3}$ (F)	ϵ (F)	c (F)	$cA^{-1/3}$ (F)	ϵ (F)
Mg	2.87 ± 0.12	0.99	0.545	2.98	1.03	0.591
Cu	4.38 ± 0.08	1.09	0.545	4.27	1.07	0.568
Ag	5.34 ± 0.06	1.12	0.545	5.15	1.08	0.522
In	5.53 ± 0.08	1.14	0.545	5.24	1.08	0.522
Au	6.74 ± 0.06	1.16	0.545	6.38	1.10	0.547
Pb	6.87 ± 0.04	1.16	0.545	6.50	1.10	0.547

TABLE V. A-dependence fits. The fitting parameters are $\gamma_\rho^2/4\pi$ and $\sigma_{\rho N}$ for each energy and for each set of nuclear parameters. The values $\alpha_{\rho\rho}$ are taken from Ref. 14. $|f_0|^2$ is the one-nucleon cross section derived from the fits, and may be compared to the measured hydrogen cross sections listed in Table III.

E_ρ (GeV)	Nuclear parameters	$\alpha_{\rho\rho}$	$\gamma_\rho^2/4\pi$	$\sigma_{\rho N}$ (mb)	$\lvert f_0\rvert^2$ (μb/GeV^2)
8.8	Best fit	−0.24	0.68 ± 0.04	26.8 ± 1.2	105 ± 11
	E-S	−0.24	0.63 ± 0.04	25.9 ± 1.0	106 ± 11
6.5	Best fit	−0.27	0.74 ± 0.04	30.1 ± 1.5	124 ± 15
	E-S	−0.27	0.65 ± 0.05	27.9 ± 1.3	120 ± 15
6.1	Best fit	−0.27	0.58 ± 0.03	26.1 ± 0.9	117 ± 10
	E-S	−0.27	0.62 ± 0.04	27.5 ± 1.1	122 ± 13

photoproduction to fit measured neutron-nucleus and proton-nucleus total cross sections.[3] Thus by using a consistent optical model for both ρ^0 photoproduction and nucleon-nucleus scattering, we expect that uncertainties due to nuclear parameters will be minimized. The "E-S" parameters are those obtained from electron-scattering experiments.[4] Note that the $\theta = 0$ cross sections in Table II are obtained from the measured rates by using a particular set of parameters.

The results of the A-dependence fits are listed in Table V. Typical fits to the data are shown in Fig. 6. In Fig. 7 we show explicitly the variation of the parameters $\gamma_\rho^2/4\pi$ and $\sigma_{\rho N}$ with $\alpha_{\rho\rho}$. Also listed in Table V are the values of $|f_0|^2$ obtained for each fit. These are plotted with the directly measured hydrogen cross sections in Fig. 4.

III. CONCLUSIONS

The present results agree well with recent determinations of $\gamma_\rho^2/4\pi$ and $\sigma_{\rho N}$ obtained from elastic ρ-photoproduction on deuterons at SLAC.[16] The DESY-MIT results[17] at 6.5 GeV are consistent with the present results. However, the data on production from hydrogen show significant disagreement with results from the SLAC bubble chamber,[11] where the observed hydrogen cross section at 4.7 GeV is given by $(d\sigma/dt)_H = (80 \pm 5)\exp[(5.5 \pm 0.3)t]$ μb/GeV^2. This is to be compared with the results of this experiment at 5.6 GeV: $(d\sigma/dt)_H = (134 \pm 10) \times \exp[(8.6 \pm 0.5)t]$ μb/GeV^2. Some of this discrepancy is due to different methods of analysis, but a real discrepancy in the raw cross sections undoubtedly remains.

ACKNOWLEDGMENTS

The authors wish to thank Professor Donald Yennie and Professor Kurt Gottfried for several illuminating discussions during the course of these experiments. The success of the program is largely due to the efficient operation of the Cornell Synchrotron under the direction of Dr. M. Tigner.

---

*Work supported by the National Science Foundation.

†Present address: Department of Physics, University of Maryland, College Park, Maryland 20742.

‡Present address: Western Electric Company, Engineering Center, P.O. Box 900, Princeton, New Jersey 08540.

§Present address: Laboratori Nazionali di Frascati, Casella Postale N. 70, 00044 Frascati (Roma), Italy.

‖Present address: Department of Physics, University of Essex, Wivenhoe Park, Colchester, Essex, England.

[1]G. McClellan *et al.*, Phys. Rev. Letters 22, 374 (1969); H. Ogren, Ph.D. thesis, Cornell University, 1970 (unpublished).

[2]P. Söding, Phys. Letters 19, 702 (1966).

[3]J. Engler *et al.*, Phys. Letters 28B, 64 (1968); 29B, 321 (1969); G. Bellettini *et al.*, Nucl. Phys. 79, 609 (1966); E. F. Parker and L. W. Jones, University of Michigan Report No. 03028-3-T, 1969 (unpublished).

[4]R. Hofstadter, Ann. Rev. Nucl. Sci. 7, 231 (1957).

[5]R. J. Glauber, in *High Energy Physics and Nuclear Structure*, edited by S. Devon (Plenum, New York, 1970), pp. 207-265.

[6]The modified Breit-Wigner resonance form used is as follows:

$$P_{BW}(m_{\pi\pi};\Gamma_0,m_\rho) = \frac{2}{\pi} m_{\pi\pi} m_\rho \Gamma(m_{\pi\pi}) \frac{1}{(m_\rho^2 - m_{\pi\pi}^2)^2 + m_\rho^2 \Gamma^2(m_{\pi\pi})},$$

where

$$\Gamma(m_{\pi\pi}) = \frac{m_\rho}{m_{\pi\pi}} \left(\frac{m_{\pi\pi}^2 - 4m_\pi^2}{m_\rho^2 - 4m_\pi^2}\right)^{3/2} \Gamma_0 .$$

[7]T. Bauer, Ph.D. thesis, Cornell University, 1970 (unpublished); Phys. Rev. D 3, 2971 (1971).

[8]D. Yennie, private communication.

[9]J. Augustin *et al.*, Lett. Nuovo Cimento 2, 214 (1969).

[10]G. Wolf, Nucl. Phys. B26, 317 (1971).
[10a]C. Berger, N. Mistry, L. Roberts, T. Talman, and P. Walstrom, Cornell Report No. CLNS-168, 1971 (unpublished).
[11]H. Bingham *et al.*, Phys. Rev. Letters 24, 955 (1970).
[12]H. Alvensleben *et al.*, Phys. Rev. Letters 23, 1058 (1969).
[13]R. L. Anderson *et al.*, Phys. Rev. D 1, 27 (1970).
[14]M. Damashek and F. Gilman, Phys. Rev. D 1, 1319 (1970).
[15]J. Trefil, Phys. Rev. 180, 1366 (1969); 180, 1379 (1969).
[16]R. L. Anderson *et al.*, paper submitted to the Fifteenth International Conference on High-Energy Physics, Kiev, U.S.S.R., 1970 (unpublished); see rapporteur talk by K. Lübelsmeyer, in *Proceedings of the Fifteenth International Conference on High-Energy Physics, Kiev, U.S.S.R., 1970* (Atomizdat, Moscow, 1971).
[17]H. Alvensleben *et al.*, Phys. Rev. Letters 24, 786 (1970).

PHYSICAL REVIEW D VOLUME 4, NUMBER 9 1 NOVEMBER 1971

Experimental Results on the Reactions $\pi^- p \to \pi\pi N$ in the c.m. Energy Range 1400–2000 MeV*

A. D. Brody,† R. J. Cashmore, A. Kernan,‡ D. W. G. S. Leith, B. G. Levi, A. Minten,† and B. C. Shen‡
Stanford Linear Accelerator Center, Stanford University, Stanford, California 94305

and

J. P. Berge,† B. Deler,§ D. J. Herndon, R. Longacre, L. R. Miller, L. R. Price,|| A. H. Rosenfeld, and P. Söding**
Lawrence Radiation Laboratory, University of California, Berkeley, California 94720
(Received 12 July 1971)

Cross sections and representative distributions are given for the reactions $\pi^- p \to \pi^+\pi^- n$, $\pi^- p \to \pi^- p\pi^0$ based on 85 000 inelastic events in the c.m. energy region 1400–2000 MeV. The angular distributions of beam, defined with respect to the final-state particles are given in terms of their moments as a function of Dalitz plot position and c.m. energy.

I. INTRODUCTION

Although the elastic and charge-exchange channels of pion-nucleon scattering experiments have been studied extensively,[1-8] the data on inelastic channels remain incomplete.[9] These channels are becoming more important since the phase-shift analyses, which have been successful in revealing the major features of the πN system, are in considerable disagreement over the detailed features of partial waves of low elasticity. For these reasons we have made systematic measurements of inelastic channels in the energy region 1400–2000 MeV.

The origin of these data are exposures of the 72-in. hydrogen bubble chamber (HBC) at Lawrence Radiation Laboratory, Berkeley, and the 30-in. HBC at Argonne National Laboratory to π^- beams in the momentum range 550–1600 MeV/c. This paper is concerned with the study of inelastic two-prong events observed in this film, i.e.,

$$\pi^- p \to \pi^+\pi^- n, \quad \sim 51\,000 \text{ events}; \tag{1}$$

$$\pi^- p \to \pi^-\pi^0 p, \quad \sim 34\,000 \text{ events}. \tag{2}$$

The other major contribution to the two-prong topology comes from elastic scattering

$$\pi^- p \to \pi^- p, \quad \sim 80\,000 \text{ events} \tag{3}$$

and this has been discussed previously.[10]

Within three c.m. energy regions, 1400–1600, 1600–1800, and 1800–2000 MeV, our data correspond to approximate μb equivalents of 0.5, 2.0, and 2.5 events per μb, respectively.

In Sec. II we describe the identification of events from reactions (1) and (2) and other details of the data analysis. In Sec. III we give cross sections for these two channels and in Sec. IV we describe the general characteristics of the reactions and give the results of moments analysis of reactions (1) and (2) throughout our entire c.m. energy region. Section V contains the results of an analysis of the $\pi^+\pi^- n$ final state leading to a presentation of the $\Delta\pi$ and ρN partial cross sections. The results of an analysis of the $\Delta^-\pi^+$ final state over a limited energy range are also summarized. Section VI contains only a short discussion of the results. The main purpose of this paper is a presentation of the experimental results. A detailed discussion of the partial-wave analyses of the inelastic data now in progress will appear at a later date.